



High-fat Diet Enhances Gastric Contractility, but Abolishes Nesfatin-1-induced Inhibition of Gastric Emptying

Zarife N Özdemir-Kumral,¹ Türkan Koyuncuoğlu,¹ Sevil Arabacı-Tamer,¹ Özlem T Çilingir-Kaya,² Ayça K Koroğlu,^{2,3} Meral Yüksel,⁴ and Berrak Ç Yeğen^{1*}

Departments of ¹Physiology and ²Histology and Embryology, Marmara University School of Medicine, Istanbul, Turkey; ³Department of Histology and Embryology, Istinye University Faculty of Medicine; Istanbul, Turkey; and ⁴Marmara University Vocational School of Health Sciences, Istanbul, Turkey

Background/Aims

Gastrointestinal motility changes contribute to development and maintenance of obesity. Nesfatin-1 (NES-1) is involved in central appetite control. The aim is to elucidate effects of NES-1 and high-fat diet (HFD) on gastrointestinal motility and to explore myenteric neuron expressions of tyrosine hydroxylase (TH), vasoactive intestinal peptide (VIP), and neuronal nitric oxide synthase (nNOS) in HFD-induced oxidative injury.

Methods

Sprague-Dawley rats were fed with normal diet (ND) or HFD. Gastric emptying rate was measured following NES-1 (5 pmol/rat, intracerebroventricular) preceded by subcutaneous injections of glucagon-like peptide 1 (GLP-1), cholecystokinin 1 (CCK-1), and gastrin/CCK-2 receptor antagonists. In carbachol-contracted gastric and ileal strips, contractile changes were recorded by adding NES-1 (0.3 nmol/L), GLP-1, CCK-1, and gastrin/CCK-2 antagonists.

Results

Neither HFD nor NES-1 changed methylcellulose emptying, but NES-1 delayed saline emptying in cannulated ND-rats. Inhibitory effect of NES-1 on gastric emptying in ND-rats was reversed by all antagonists, and abolished in HFD-rats. In HFD-rats, carbachol-induced contractility was enhanced in gastric, but inhibited in ileal strips. HFD increased body weight, while serum triglycerides, alanine transaminase, aspartate aminotransferase, glucose, and levels of malondialdehyde, glutathione, myeloperoxidase activity, and luminol-chemiluminescence in hepatic, ileal, and adipose tissues were similar in ND- and HFD-rats, but only lucigenin-chemiluminescence was increased in HFD-rats. Vasoactive intestinal peptide (VIP) and TH immunoreactivities were depressed and nNOS immunoreactivity was increased in gastric tissues of HFD-rats, while VIP and TH were enhanced, but nNOS was reduced in their intestines.

Conclusions

HFD caused mild systemic inflammation, disrupted enteric innervation, enhanced gastric contractility, inhibited ileal contractility, and eliminated inhibitory effect of NES-1 on gastric motility.

(J Neurogastroenterol Motil 2021;27:265-278)

Key Words

Cholecystokinin; Gastric emptying; Nesfatin-1; Nitric oxide synthase type I; Vasoactive intestinal peptide

Received: September 10, 2020 Revised: None Accepted: October 30, 2020

© This is an Open Access article distributed under the terms of the Creative Commons Attribution Non-Commercial License (<http://creativecommons.org/licenses/by-nc/4.0>) which permits unrestricted non-commercial use, distribution, and reproduction in any medium, provided the original work is properly cited.

*Correspondence: Berrak Ç Yeğen, MD

Department of Physiology, Marmara University School of Medicine, Basibüyük Mah. Maltepe Basibüyük Yolu No. 9/1, 34854 Maltepe, Istanbul, Turkey
Tel: +90-216-777-5627, E-mail: byegen@marmara.edu.tr

Introduction

Disturbances in the motor and sensorial activity of the gastrointestinal (GI) tract affect the life quality and cause excessive health care costs.¹ Likewise, alterations in GI motility contribute to the progress and continuation of disturbed eating habits that include obesity, which is a leading cause of overall mortality worldwide.² Based on a vast amount of literature, it was reported that rapid gastric and small intestinal motility is common in obese individuals.² Similarly, following a 2-week consumption of high-fat diet (HFD) in both rats and humans, gastric emptying (GE) rate of a fatty meal was augmented by a nutrient-specific manner, which was associated with an attenuation of GI motor and hormonal response to fat,^{3,4} resulting in delayed satiation and increased food intake.⁵ Although it was demonstrated that GE rate was not significantly changed in rats fed with HFD for 8 weeks,⁶ others have shown a slower GE rate in parallel with a reduction in plasma ghrelin, elevation in cholecystokinin (CCK) and leptin levels, which was also suggested as an adaptive hormonal response to an 8-week HFD.⁷ Research has shown that prolonged ingestion of HFD damages the enteric nervous system,^{8,9} which is well described to have a major role in controlling the GI functions via neurocrine, endocrine, and paracrine signaling mechanisms.¹⁰ HFD consumption for 20 weeks has caused injury specifically to the inhibitory motor neurons with reduced sizes of ganglionic cells and nerve bodies in the myenteric plexus of the duodenum, which was accompanied by decrease in immunoreactive density indices of vasoactive intestinal peptide (VIP), choline acetyltransferase, and neuronal nitric oxide synthase (nNOS) in the myenteric ganglia,¹¹ implicating that the enteric nervous system shows an adaptation in response to the exposure of luminal HFD for a prolonged period of time. Despite conflicting reports showing increased or decreased gastric motility, the contractile behavior of the GI smooth muscle in response to HFD has not been studied yet.

Nesfatin-1 (NES-1) is an 82-amino acid anorectic neuropeptide derived from the protein precursor nucleobindin-2 (NUCB2).¹² It is expressed in several hypothalamic and medullary areas related to appetite control (eg, supraoptic, paraventricular and arcuate nuclei, lateral hypothalamic area, and nucleus of the solitary tract), as well as in adipocytes and in the endocrine cells of the pancreas and stomach.¹²⁻¹⁵ Central or peripheral injection of NES-1 reduces food intake and weight in rats, whereas administration of its antibody stimulates food intake.¹² Expression of NES-1 in the paraventricular and supraoptic nuclei of rats was decreased due to food

deprivation, while refeeding has activated the NES-1 neurons.^{12,16} In parallel with its inhibitory effect on food intake, NES-1 was also shown to suppress the gastric contractions and motility when given centrally.¹⁷ Li et al¹⁸ have shown that the plasma levels of NES-1 were decreased when the rats were fed with HFD. Based on its regulatory role in food intake, NES-1 was postulated to be a potential therapeutic agent against obesity,¹⁹ necessitating detailed studies regarding its effects on GI contractility and motility upon the consumption of normal diet (ND) or HFD. The primary aim of the present study is to explore the impact of HFD on GE rate, and gastric and intestinal contractility. The secondary aim is to evaluate the effect of NES-1 on GE rate and contractility of gastric and ileal strips obtained from rats fed with ND and HFD, and the involvement of CCK-1, CCK-2, and glucagon-like peptide 1 (GLP-1) receptors in these responses. Another aim is to elucidate the contribution of HFD-induced oxidative injury and the alterations in the expressions of tyrosine hydroxylase (TH), VIP, and nNOS in the myenteric neurons of the rats fed with ND or HFD.

Materials and Methods

Animals

Male Sprague-Dawley rats (230-290 g, 10-week-old) were supplied by the Marmara University Animal Center, housed in a humidity- (65-70%) and temperature-controlled ($22 \pm 2^\circ\text{C}$) room with exposure to artificial light from 7 AM to 7 PM. Rats were fed with ND (2.7 % fat, $n = 24$) or HFD (45% fat, $n = 24$) and received tap water ad libitum for 8-12 weeks. All the experiments were performed by following the guidelines of the New York Academy of Sciences and the Turkish law on the use of animals in experiments. The project was approved by the Marmara University Animal Ethics Committee (Date: 2.05.2017; Approval no: 37.2017.mar).

Experimental Design

The study consisted of 2 separate experimental groups. In both Experiment 1 (E-1) and Experiment 2 (E-2), rats had intracerebroventricular (ICV) cannula placements on the 7th week of the feeding period, while Gregory cannula installation was made on the 5th week in the rats of E-2 (Fig. 1). In the E-1 group, at the end of the 8 weeks, gastric emptying of methylcellulose test was performed, and blood, liver, ileum, and adipose tissues were obtained for the assessment of metabolic and oxidative states of the groups fed with ND or HFD. The rats of the E-2 group had emptying sessions

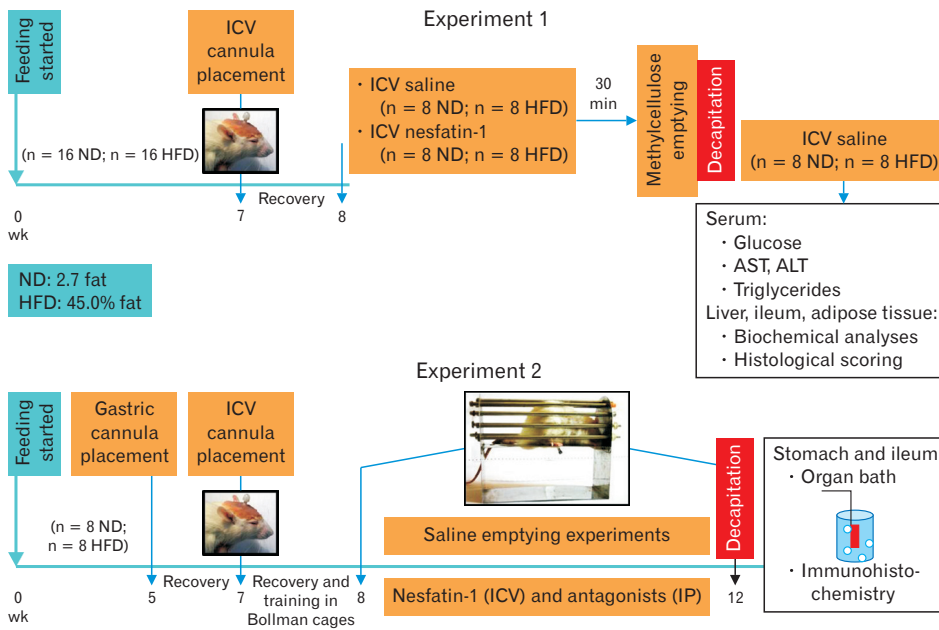


Figure 1. The design and the time course of the experimental procedures. ND, normal diet; HFD, high-fat diet; ICV, intracerebroventricular; IP, intraperitoneal; AST, aspartate aminotransferase; ALT, alanine transaminase.

every other day for a 4-week period, starting by the end of the 8th week. On the 12th week, gastric and ileal strips of the E-2 rats were mounted in *in vitro* organ baths, while samples of gastric and ileal tissues were obtained for immunohistochemistry.

Implantation of Intracerebroventricular Cannulas

In all rats of both experimental groups, ICV cannulas were placed on the 7th week for the injections of NES-1 (0.05 $\mu\text{g}/\text{rat}$ = 5 pmol/rat; NES-1 (1-82) rat; Cat. No. 003-22B; Phoenix Pharmaceuticals Inc, USA) or saline (0.5 $\mu\text{L}/\text{rat}$). The dose of NES-1 was based on a previous study that has shown the inhibitory effect of NES-1 on food intake and GE.²⁰ The rats were anesthetized with ketamine and chlorpromazine cocktail (100 mg/kg and 10 mg/kg, intraperitoneally), and body temperature was kept at $\sim 37^{\circ}\text{C}$. Rats were fixed in a stereotaxic apparatus (Stoelting, Wood Dale, IL, USA) with the head flat, and holes were drilled for the implantation of cannula guides (22-gauge; Plastic Products, Roanoke, VA, USA). The cannulas were inserted at 1 mm above the target location (anterior/posterior [A/P], -3.30 mm; lateral [L], ± 0.0 mm; and dorsal/ventral [D/V], -3.8 mm), secured with dental cement (Croform acrylic powder and cold liquid) and stabilized by 2 skull screws.²¹ A dummy cannula (Plastics One Canula C313DC Roanoke, VA, USA) was placed in each of the guides to prevent clogging. All ICV injections were made in a 5- μL volume over a period of 100 seconds using a Hamilton syringe. At the end of the experiments, verification of the ICV cannula placement was made by methylene blue injection.

Gastric Emptying of Methylcellulose Liquid Meal

Following a 1-week recovery period after stereotaxic surgery, GE of a liquid meal containing methylcellulose was measured in E-1 rats (Fig. 1).²² Methylcellulose and phenol red (50 mg/100 mL), which is a dilution marker that cannot be absorbed, were mixed in water and stirred continuously at 37°C . After an overnight fasting, NES-1 (5 pmol/0.5 μL) or saline (0.5 μL) was injected, and 5 minutes later, 1.5 mL of methylcellulose was given by gavage through a polyethylene tube. Thirty minutes after the administration of methylcellulose, rats were decapitated, and the stomachs were clamped and dissected at the pylorus and cardia ends. The trunk blood was collected for the measurement of glucose, triglyceride, alanine transaminase (ALT), and aspartate aminotransferase (AST) levels in the serum. After the stomachs were homogenized in NaOH (0.1 M), suspensions were let to settle for an hour, supernatant (5 mL) was taken and mixed with trichloroacetic acid (20% weight/volume; 0.5 mL). The samples were centrifuged (2800 rpm, 20 minutes) and NaOH (0.5 M; 4 mL) was added to the supernatant and read spectrophotometrically at 560 nm. Percentage of GE was calculated according to the formula: $\text{GE} = 1 - (\text{absorbance of test stomach} / \text{average absorbance of 2 standard stomachs}) \times 100$; where the standard stomachs were obtained from 2 rats killed immediately after the meal administration.²² Then, the liver, ileum and adipose tissues were removed to determine lipid peroxidation, glutathione (GSH) and chemiluminescence levels, myeloperoxidase (MPO) activity, and histological damage scores of rats fed with ND

or HFD for 8 weeks.

Gregory Cannula Installation and Determination of Gastric Emptying Rate

Rats in the E-2 were initially equipped with gastric cannulas at 2 weeks before ICV cannula placement (Fig. 1). After fasting for 18 hours, rats were anesthetized with ketamine plus chlorpromazine given intraperitoneally. A paramedian incision was made and a Gregory cannula was installed at the anterior corpus, which was exteriorized through a midline incision.²³ The incisions were closed in layers and the rats were then housed individually. During the following 3 weeks, animals were allowed to recover from both operations, and were trained to sit in Bollman-type cages. Starting by the 8th week, rats were fasted overnight for the emptying sessions held in Bollman cages every other day. The stomach was flushed with warm (37°C) saline until clean. Three-milliliter saline containing phenol red (60 mg/L, pH was adjusted to 7.0) as a non-absorbable dilution marker was instilled through the gastric fistula. After 5 minutes of the instillation of the saline via a polyethylene-tube connected to the cannula, the tube was pulled to collect the residual gastric content for 1 minute. GE was determined from the recovered volume and phenol red concentrations, as reported previously.²⁴ Phenol red concentration was determined spectrophotometrically from the absorbance read at 550 nm. The absorbance (A_1 : absorbance of instilled solution; A_2 : absorbance of collected fluid) and the volumes (V_1 : volume of instilled solution; V_2 : volume of collected fluid) were used in the following formula, and the GE rate (GE; mL/5 min) was calculated as: $GE = (V_1 \times A_1) - (V_2 \times A_2) / (A_1 + A_2) / 2$.²⁴

GE experiments were commenced 5 minutes after ICV NES-1 (5 pmol/0.5 μ L) or saline (0.5 μ L) injection, which were preceded (5 minutes before) with subcutaneous injections of either saline or GLP-1 receptor antagonist exendin 9-39 (30 μ g/kg; Sigma, St Louis, MO, USA) or CCK-1 receptor antagonist devazepide (1 mg/kg; Sigma) or gastrin/CCK-2 receptor antagonist YM022 (1 mg/kg; Sigma). The antagonists were freshly dissolved in saline (exendin 9-39) or dissolved in dimethyl sulfoxide (devazepide and YM022) and diluted with saline. The emptying of physiological saline with different drug applications was studied in a random order, and was repeated at least 3 times in each animal, and the average of repeated tests was taken as the emptying result for each rat. Routinely, at least 30 minutes was allowed between emptying tests.

Assessment of Gastric and Ileal Contractility

At the end of the 12 weeks, cannulated stomachs and ileal tis-

ues of the E-2 rats were removed following decapitation. The stomach was opened along the great curvature, rinsed with Krebs solution and the posterior gastric corpus was cut along the longitudinal axis, while a 3-cm length of ileum was removed from an area 10 cm proximal to the ileocecal junction. Gastric ($\sim 6 \times 3$ mm, longitudinal) and ileal (~ 15 mm, circular) strips were mounted vertically with 4.0 silk between 2 curved hooks and placed into 20-mL organ baths, which were aerated with a mixture of 95% O₂ and 5% CO₂ containing Krebs–Henseleit buffer solution (pH 7.4, 37°C, composition in mmol/L: NaCl, 118; CaCl₂, 1.8; KCl, 4.8; MgSO₄, 1.2; NaHCO₃, 25; KH₂PO₄, 1.2; glucose, 11). The continuous dynamic curves were recorded with isometric force transducers (IOBS 99 isolated tissue bath stand sets; Commat Ltd, Ankara, Turkey) and visualized with MP 35 data acquisition system (BIOPAC Systems, Inc, Goleta, CA, USA). After a 60-minute equilibration period interrupted with washouts at every 20 minutes, the strip was then pre-loaded at an initial stretch of 1 g.

At the beginning of each experiment, 3×10^{-6} mM carbachol (CCh) was added to the tissue chamber and the baseline contractile response of each strip was obtained. Then, after refreshing the solution, first NES-1 (0.1, 0.3, or 1 nmol/L) was added in the chamber for a 5-minute preincubation, and it was followed by CCh addition. Following the dose-response experiments, the mid-dose (0.3 nmol/L, nearly equivalent to 20 times the in vivo dose) of NES-1 was chosen for the rest of the study. After a 30-minute washout period, the strips were pre-incubated for 5 minutes with NES-1 (0.3 nmol/L) plus exendin (30 nmol/L) or devazepide (30 nmol/L) or YM022 (30 nmol/L), and CCh was added to record the contractile responses. At the end of each experiment, tissue wet weights were measured and the amplitudes of the contractions recorded at each step were defined as g/100 mg wet tissue weight. The doses of the used antagonists were based on previous reports.²⁵

Biochemical Analyses

Serum levels of ALT, AST, triglycerides, and glucose were determined by colorimetric assay using a Clinical System 700 analyser (Beckman Instruments, Brea, CA, USA).

Measurement of Hepatic, Intestinal, and Adipose Tissue Myeloperoxidase Activity

Tissue MPO activity, which shows a positive correlation with the microscopically counted neutrophil content, is commonly utilized to assess the neutrophil infiltration in inflamed tissues.²⁶ For this purpose, liver, ileum, and adipose tissue samples were homogenized in hexadecyltrimethylammonium bromide (HETAB)

and centrifuged at 12 000 rpm and 4°C for 10 minutes. Then the pellet was re-homogenized in HETAB and EDTA (10 mM; Sigma Chemical Co, St. Louis, MO, USA). The hydrogen peroxide-dependent oxidation of *o*-Dianisidine dihydrochloride (C₁₄H₁₆N₂O₂ · 2HCl), measured at 460 nm of spectrophotometer, was used to determine MPO activity, and it was expressed as unit per g of tissues.

Measurement of Hepatic, Intestinal, and Adipose Tissue Malondialdehyde and Glutathione Levels

Homogenized (Ultra Turrax; IKA, Staufen, Germany) tissue samples (in 10% trichloroacetic acid) were centrifuged at 3000 g and 4°C for 15 minutes. Supernatant was removed and further centrifuged at 10 000 g for 8 minutes. As lipid peroxidation by-products, malondialdehyde (MDA) levels (U/g tissue) were determined from the generation of thiobarbituric acid-reactive substances.²⁷ Using a modified Ellman procedure, antioxidant GSH levels (nmol/g tissue) were determined.²⁸

Measurement of Hepatic, Intestinal, and Adipose Tissue Luminol- and Lucigenin-enhanced Chemiluminescence Levels

In order to measure the generation of reactive oxygen metabolites (ROM), chemiluminescence (CL) assay is commonly used. Based on a non-invasive technique, in which probes are used as enhancers, superoxide radical is detected by the lucigenin probe, while the other radicals (hydroxyl radical, hydrogen peroxide, and hypochlorous acid) are measured by using the luminol probe.²⁹ Luminescence of the samples was recorded at room temperature

by a luminometer (Mini Lumat LB 9509; EG&G Berthold Technologies GmbH & Co. KG, Bad Wildbad, Germany) after the addition of luminol or lucigenin (0.2 mM in each) probes. CL levels were then expressed as area under the curve of relative light unit per mg of tissues.³⁰

Histological Analyses

Liver and small intestine samples obtained from all experimental groups were fixed in 10% neutral buffered formalin, and routine histological assessments were applied for light microscopic examinations. Briefly, tissues were dehydrated in ascending alcohol series (70%, 90%, 96%, and 100%), cleared with xylene and embedded in paraffin. Paraffin tissue blocks were cut at 5- μ m thickness by rotary microtome (Leica RM2125RT, Wetzlar, Germany) and placed on glass slides. Sections were stained with H&E for histopathological analyses, while liver sections were also stained with Gomori's trichrome technique to analyze the changes in connective tissue. Using a semiquantitative scale (0: none, 1: mild, 2: moderate, and 3: severe), tissues of the E-1 group were histopathologically evaluated at \times 200 magnification. The scoring parameters for the liver were (1) hepatocyte ballooning, (2) apoptotic cells, (3) fibrosis, (4) increased number/hypertrophy of Kupffer cells, (5) vascular congestion/dilation, (6) neutrophil infiltration, and (7) steatosis. The intestinal tissues were scored in terms of (1) neutrophil infiltration, (2) epithelial cell degeneration/ epithelial hyperplasia, (3) loss of Goblet cells, (4) vascular congestion, (5) villi loss, and (6) irregular villi. The maximum scores were 21 and 18 for the liver and intestinal tissues, respectively,³¹ and at least 5 areas were scored in each of the tissue samples.

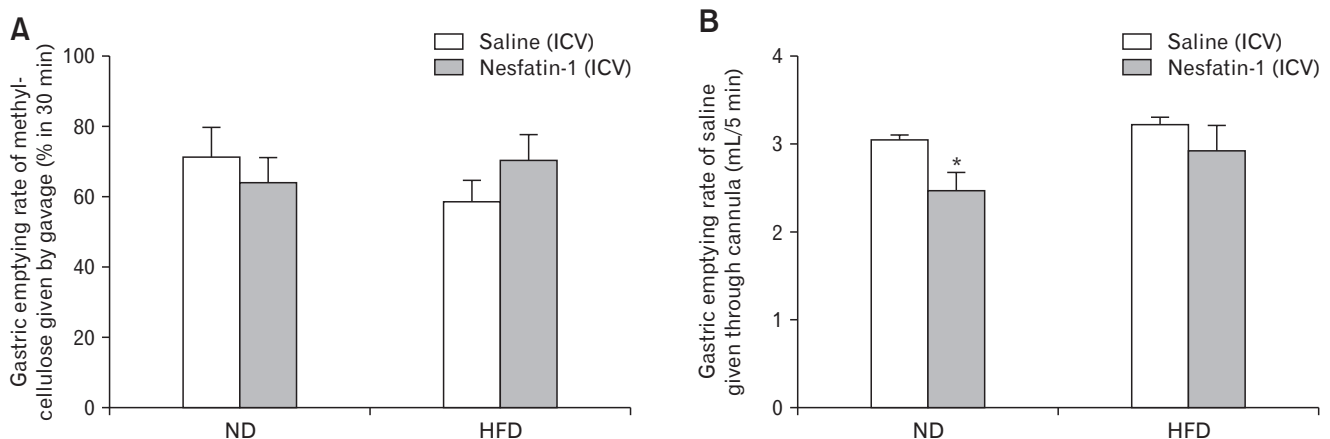


Figure 2. Gastric emptying rate of (A) methylcellulose (%; 30 minutes) and (B) saline (mL/5 min) after the intracerebroventricular (ICV) administration of saline (n = 8) or nesfatin-1 (5 pmol/rat, n = 8) in rats fed with normal diet (ND; n = 8) or high-fat diet (HFD; n = 8). **P* < 0.05, compared to ND + saline-administered group.

For immunohistochemical analyses, the tissue sections of the E-2 group were labelled with anti-TH (P40101-150; Pel-Freez, Rogers, AR, USA), anti-nNOS (ab1376; Abcam, Cambridge, MA, USA), and anti-VIP (ab78536; Abcam, Cambridge, MA, USA) antibodies, while 3,3'-Diaminobenzidine was used as a chromogen for all immunohistochemical labelings. All slides were examined and photographed by light microscope (BX51; Olym-

pus, Tokyo, Japan) with a digital camera (DP72; Olympus, Tokyo, Japan).

Statistical Methods

The results are expressed as the mean ± SEM. One-way ANOVA and Tukey-Kramer multiple comparison tests were used to evaluate the level of statistical significance (Prism 9.0; GraphPad,

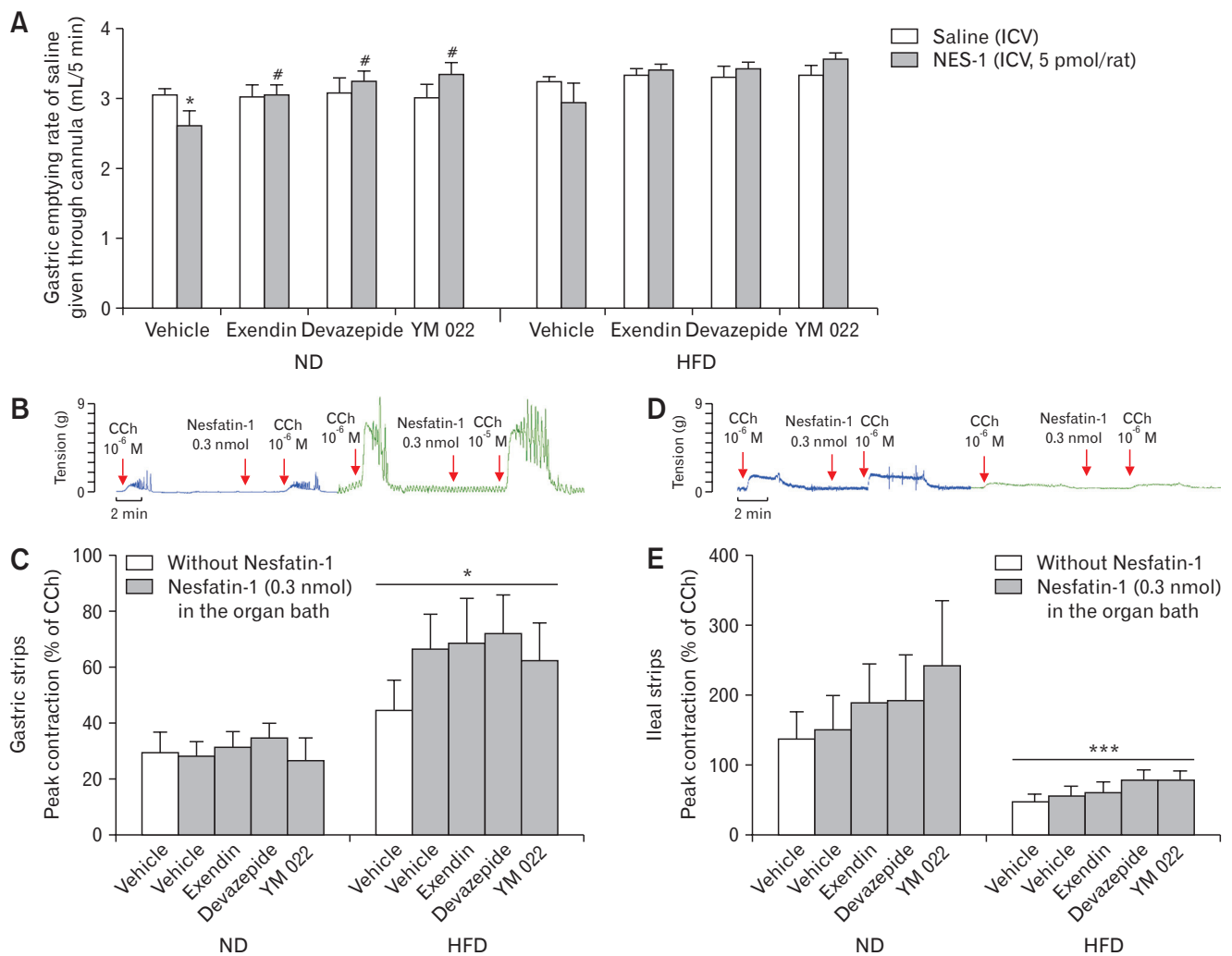


Figure 3. The effect of the antagonists on gastric emptying rate, gastric contractions, and ileal contractions. (A) Gastric emptying rate of saline (mL/5 min) in rats fed with normal diet (ND; n = 8) or high-fat diet (HFD; n = 8). After intraperitoneal (IP) injection with glucagon-like peptide 1 (GLP-1) antagonist (exendin), cholecystikinin 1 (CCK-1) antagonist (devazepide), CCK-2 antagonist (YM022), or vehicle (saline/dimethyl sulfoxide), saline or nesfatin-1 (NES-1; 5 pmol/rat) was administered intracerebroventricularly (ICV), **P* < 0.05 compared to ICV saline-treated group, #*P* < 0.05, compared to ICV NES-1 + IP vehicle-treated group; (B) Representative peak contractions in response to the submaximal dose of carbachol (CCh), recorded from the gastric strips of rats fed with ND or HFD; (C) The average peak contractions of gastric strips in response to the submaximal dose of CCh with the absence or presence of NES-1, exendin, devazepide, YM022, or vehicle in the organ bath, **P* < 0.05, compared to ND-fed groups; (D) Representative peak contractions in response to the submaximal dose of CCh, recorded from the ileal strips of rats fed with ND or HFD; (E) The average peak contractions of ileal strips in response to the submaximal dose of CCh with the absence or presence of NES-1, devazepide, YM022, or vehicle in the organ bath, ****P* < 0.001, compared to ND-fed groups.

San Diego, CA, USA). Values of $P < 0.05$ were considered as significant.

Results

Changes in Gastric and Intestinal Motility

As compared to ND-fed rats ($72.1 \pm 8.1\%$), GE rate of methylcellulose in a 30-minute period was not significantly altered when rats were fed with HFD for 8 weeks ($59.3 \pm 5.9\%$), but a tendency to a delayed GE was observed (Fig. 2A). Centrally administered NES-1 did not significantly change methylcellulose emptying in either ND-fed ($64.6 \pm 7.1\%$) or HFD-fed ($70.8 \pm 7.2\%$) rats. GE rate of saline at 5 minutes following its instillation through the gastric cannula was similar in rats fed with ND (3.07 ± 0.03 mL/5 min) or HFD (3.25 ± 0.06 mL/5 min; Fig. 2B). However, ICV administration of NES-1 significantly delayed GE of saline (2.49 ± 0.19 mL/5 min) in ND-fed cannulated rats as compared to ICV saline ($P < 0.05$), but NES-1-induced delay was abolished in the HFD-fed rats with the gastric cannulae (2.95 ± 0.27 mL/5 min).

In the next setup of experiments with the cannulated rats, GLP-1 receptor antagonist exendin 9-39, CCK-1 receptor antagonist devazepide, or gastrin/CCK-2 receptor antagonist YM022 was injected peripherally before the ICV administration of saline or NES-1 (Fig. 3). None of the antagonists changed the saline emptying rate in ICV saline-administered rats, but NES-1-induced delay (2.49 ± 0.19 mL/5 min) was abolished by the receptor antagonist of GLP-1 (3.06 ± 0.13 mL/5 min, $P < 0.05$), CCK-1 (3.25 ± 0.13 mL/5 min, $P < 0.05$) or CCK-2 (3.35 ± 0.13 mL/5 min, $P < 0.05$) in ND-fed rats (Fig. 3A). In HFD-fed rats, in which ICV NES-1 per se has not altered GE significantly, none of the antagonists had an effect on the GE rate of saline.

In response to the submaximal dose of CCh, contractility changes induced by NES-1 and antagonists were recorded in the gastric and ileal strips mounted in isolated organ baths. In the gastric segments of HFD-fed rats, a significant elevation was present in the peak contractions as compared to those of ND-fed rats ($P < 0.05$), while the CCh-induced peak contractions of the ileal strips were depressed in the HFD-rats ($P < 0.001$; Fig. 3). On the other hand, the latent period between the addition of CCh and contraction in gastric and ileal tissues was not changed with the diet type (data not shown). Despite that NES-1 had no significant impact on the peak contractions of the gastric or ileal smooth muscles of rats fed with either ND or HFD, the contractile states following the addition of CCh were prolonged by 4.8 ± 0.2 minutes in HFD-rats

as compared to ND-rats. Moreover, addition of any of the antagonists into the organ bath did not have a significant effect on diet- or NES-1-induced changes.

Biochemical and Histological Analysis of Tissues

Feeding rats with HFD for 8 weeks increased the body weight significantly with respect to ND-fed rats ($P < 0.01$; Table), but serum levels of AST, ALT, glucose, and triglyceride were similar in the 2 groups with different diet regimes. To assess the contribution of HFD-induced inflammation and oxidative injury in the development of GI motility changes, MPO, MDA, GSH, luminol-, and

Table. Body Weight, Serum Levels of Alanine Transaminase, Aspartate Aminotransferase, Glucose, and Triglycerides and Levels of Malondialdehyde, Glutathione, Luminol/Lucigenin-enhanced Chemiluminescence, and Myeloperoxidase Activity in the Liver, Ileum, and Adipose Tissues of Rats Fed With Normal Diet or High-fat Diet for 8 Weeks.

Parameters	ND (n = 8)	HFD (n = 8)
Body weight (g)		
Week 0	281.20 \pm 4.60	250.20 \pm 8.80
Week 8	295.80 \pm 6.00	320.40 \pm 6.73 ^a
AST (U/L)	173.20 \pm 12.40	170.50 \pm 10.40
ALT (U/L)	35.00 \pm 2.30	31.00 \pm 1.00
Glucose (mg/dL)	103.00 \pm 1.80	125.70 \pm 10.30
Triglyceride (mg/dL)	62.20 \pm 6.80	53.20 \pm 4.90
Liver		
MDA (nmol/g)	6.55 \pm 0.55	9.47 \pm 1.79
GSH (μ mol/g)	2.37 \pm 0.07	2.18 \pm 0.08
Luminol (rlu/mg)	12.40 \pm 4.65	13.00 \pm 1.20
Lucigenin (rlu/mg)	8.34 \pm 1.45	14.98 \pm 1.17 ^b
MPO (U/g)	15.5 \pm 3.16	16.49 \pm 2.65
Ileum		
MDA (nmol/g)	8.70 \pm 2.71	7.22 \pm 1.63
GSH (μ mol/g)	1.17 \pm 0.12	1.05 \pm 0.09
Luminol (rlu/mg)	18.48 \pm 1.92	25.64 \pm 6.38
Lucigenin (rlu/mg)	13.28 \pm 2.57	28.26 \pm 4.48 ^b
MPO (U/g)	114.70 \pm 15.56	107.90 \pm 17.72
Adipose		
MDA (nmol/g)	5.40 \pm 1.58	8.34 \pm 3.95
GSH (μ mol/g)	0.38 \pm 0.11	0.33 \pm 0.07
Luminol (rlu/mg)	5.40 \pm 1.21	8.78 \pm 1.21
Lucigenin (rlu/mg)	6.24 \pm 1.32	11.66 \pm 1.67 ^b
MPO (U/g)	19.48 \pm 2.23	18.00 \pm 3.76

ND, normal diet; HFD, high-fat diet; AST, aspartate aminotransferase; ALT, alanine transaminase; MDA, malondialdehyde; GSH, glutathione; MPO, myeloperoxidase.

Data are expressed as mean \pm SEM.

^a $P < 0.01$, compared to week 0; ^b $P < 0.05$, compared to ND group.

lucigenin-enhanced CL levels were evaluated in the adipose, ileum, and liver tissues (Table). Despite a tendency to increased MDA levels observed in the hepatic and adipose tissues of the HFD group, levels of GSH, MPO, and luminol CL were not different between the tissues of ND- and HFD-fed rats. On the other hand, lucigenin-enhanced CL, indicative of superoxide anion, was significantly increased in all 3 tissues of the HFD group as compared to those of the ND-fed rats ($P < 0.05$).

When compared to regular morphology of the liver parenchyme in the ND group, vascular congestion, neutrophil infiltration, fatty vacuoles, and ballooning of hepatocytes were seen in the hepatic tissues of rats fed with HFD for 8 weeks (Fig. 4). Intestinal tissues of the ND group showed regular histological appearance with proper epithelial lining; whereas hypertrophied epithelial cells, vascular congestion, and abnormal intestinal glands were evidenced in the intestines of the HFD group. The scoring of these features

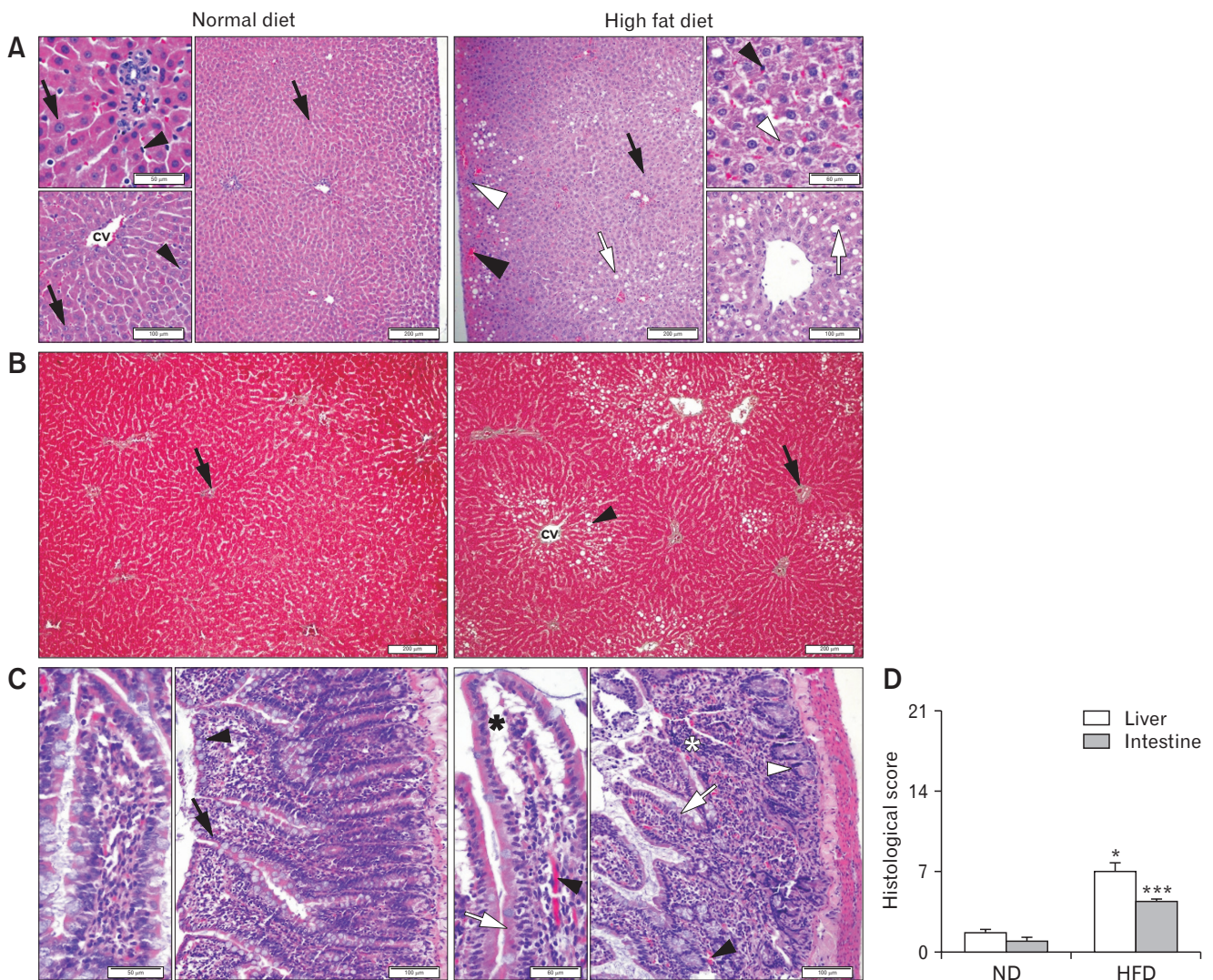


Figure 4. Representative micrographs of the liver tissue stained with (A) H&E (black arrow, hepatocyte with regular morphology; black arrowhead, Kupffer cell; white arrow, fatty vacuoles in liver parenchyme; white arrowhead, hepatocyte with ballooning). Central vein (CV) and (B) Gomori's trichrome (black arrow, connective tissue stained in green color; black arrowhead, fatty vacuoles in liver parenchyme). (C) Representative micrographs of the intestine tissue in the normal diet (ND) (black arrow, epithelial cells with normal morphology; black arrowhead, Goblet cell) and high-fat diet (HFD) (black asterisk, vascular congestion; black arrowhead, congestive regions; white asterisk, neutrophil infiltration; white arrow, hypertrophied epithelial cells; white arrowhead, intestinal gland with abnormal appearance) groups. Stained with H&E. Bars showing 100 μm and 50 μm (insets). (D) Histological damage scores in the liver and intestines of rats fed with ND or HFD. * $P < 0.05$, *** $P < 0.001$, compared to the corresponding tissue of the ND-fed group.

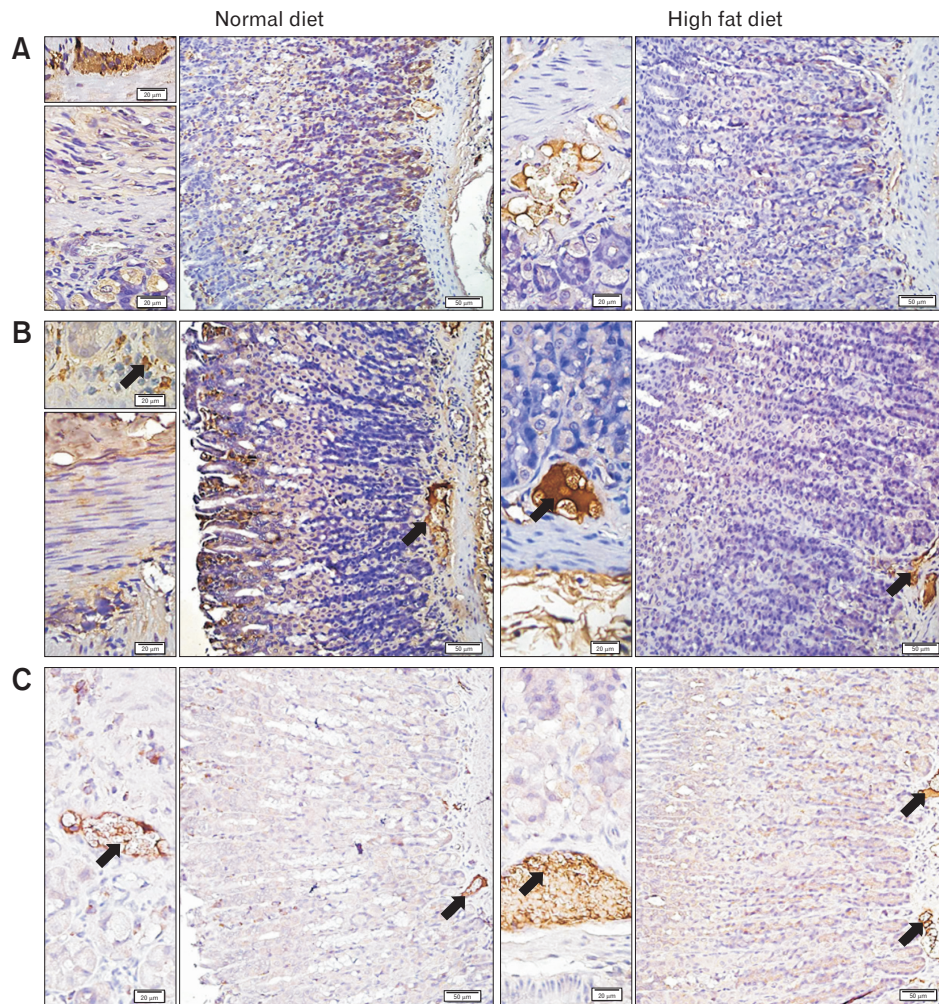


Figure 5. Representative micrographs of the gastric tissues labeled with (A) tyrosine hydroxylase (TH), (B) vasoactive intestinal peptide (VIP), and (C) neuronal nitric oxide synthase (nNOS), where brown-stained regions (arrow) indicate the positive immunoreactivities. TH immunoreactivity was observed in the myenteric/submucosal plexuses and glandular structures, VIP immunoreactivity was more distinct in epithelial linings and myenteric plexus, while nNOS immunoreactivity was detected mainly in the myenteric nerve plexus of the stomach. Bars showing 50 μm and 20 μm (insets).

revealed that both hepatic and intestinal tissues of the HFD-rats presented with higher histological scores, indicative of mild inflammation ($P < 0.05$ and $P < 0.001$; respectively).

In order to associate a possible change in the expression of neurotransmitters with the ingestion of HFD, immunoreactivity studies were carried out in the gastric and ileal tissues. In the gastric tissues of HFD-fed group, TH and VIP immunoreactivities were relatively less when compared to ND group, while the nNOS immunoreactivity showed a tendency to increase in the gastric tissues of HFD group (Fig. 5). On the other hand, the changes in the immunoreactivities of the intestinal tissues showed the opposite (Fig. 6). In the ileal tissues of the HFD-fed rats, both TH and VIP immu-

noreactivities were elevated with a concomitant reduction in nNOS immunoreactivity.

Discussion

The present findings demonstrated that a prolonged feeding with HFD did not change the GE rate of non-nutrient liquids, but the inhibitory effect of centrally administered NES-1 on the early period of liquid emptying in ND-fed rats was abolished when the rats were previously fed with HFD. On the other hand, peripheral administration of GLP-1 as well as CCK-1 and CCK-2 receptor antagonists reversed NES-1-induced delay in the GE of ND-fed

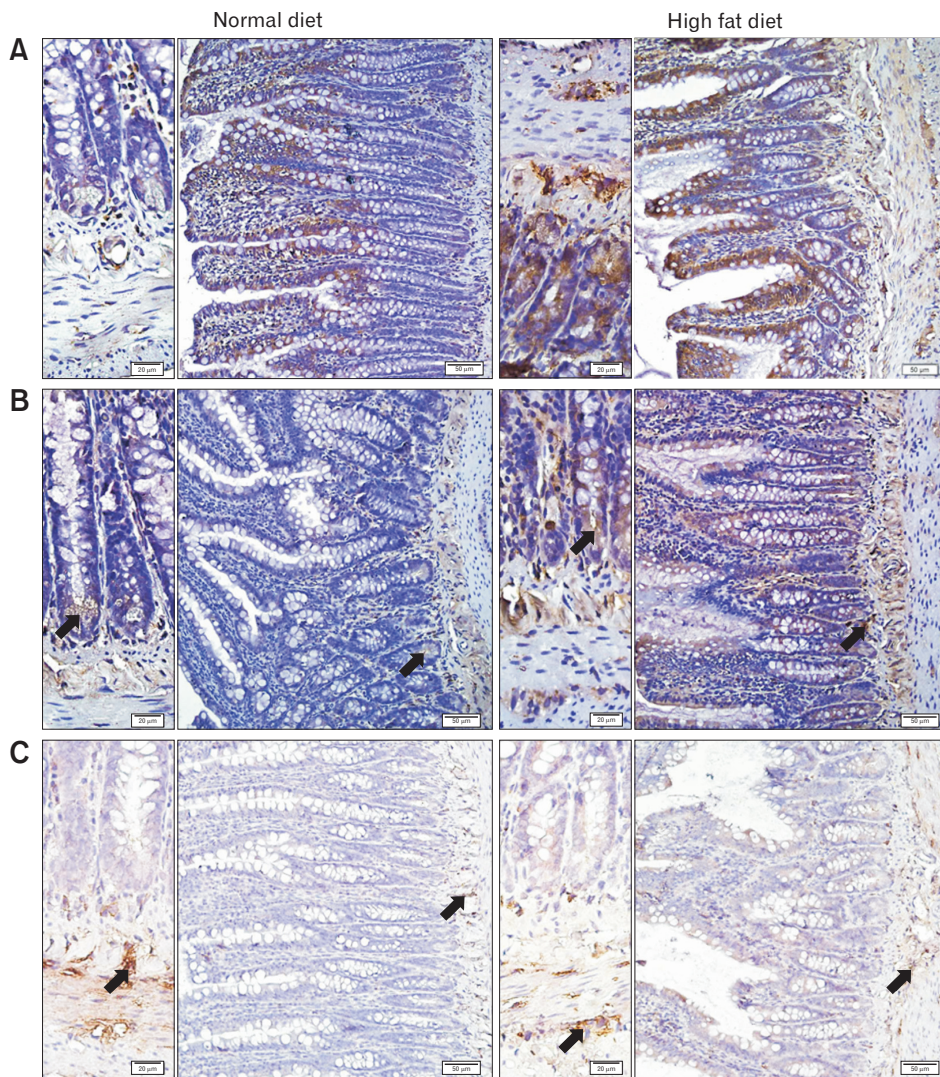


Figure 6. Representative micrographs of the ileal tissues labeled with (A) tyrosine hydroxylase (TH), (B) vasoactive intestinal peptide (VIP), and (C) neuronal nitric oxide synthase (nNOS), where brown-stained regions (arrow) indicate the positive immunoreactivities. TH immunoreactivity was more distinct in the epithelial linings and myenteric plexus, VIP immunoreactivity was detected in epithelial linings and myenteric plexus and nNOS immunoreactivity was observed in the myenteric nerve plexus of the intestines. Bars showing 50 μm and 20 μm (insets).

rats. In the *in vitro* conditions, contractile response to cholinergic stimulation was enhanced in the gastric strips of HFD-rats along with an inhibition of the ileal contractility. Although the presence of NES-1 in the organ bath did not change the maximum amplitude of CCh-induced contractions in either ND- or HFD-rats, a sustained contractile state for a longer period was noted with the addition of NES-1. HFD-fed rats with altered gastric and intestinal contractility also showed a mild inflammation of the hepatic, ileal, and adipose tissues along with a significant body weight gain. Moreover, VIP immunoreactivity and TH immunoreactivity, indicative of the VIPergic and noradrenergic/dopaminergic neurons,

were depressed in the gastric tissues, but their intensities were enhanced in the intestines of rats fed with HFD. On the other hand, nNOS immunoreactivity was increased in the gastric neuronal layers, but reduced in the intestines of the HFD-fed rats. Thus, HFD feeding, which causes a systemic inflammation and disrupts the interbalance of enteric innervation, enhances gastric smooth muscle contractility, inhibits ileal smooth muscle contractility, and eliminates the inhibitory effect of NES-1 on gastric motility.

In obese people, the size of the stomach during the fasting or post-prandial states was found to be similar to that of the normal individuals, suggesting that obesity does not change gastric capac-

ity and accommodation.³² However, several studies have reported that obese patients demonstrate an accelerated GE,^{33,34} while other studies have indicated that obese patients develop a decline in motility by aging, which is attributed to the development of insulin-resistance and accumulation of excessive fat.³⁵ There is extensive evidence that NES-1 inhibits gastric functions in ND conditions. Our data revealed that feeding with HFD, in one hand, increased the contractility of gastric smooth muscle in response to cholinergic stimulation. On the other hand, the delay in GE due to centrally administered NES-1, which could be abolished by either CCK or GLP-1 receptor antagonists, was lost in HFD-fed rats. When mice or rats were at a normal diet, it was shown that centrally administered NES-1 inhibited gastroduodenal motility and suppressed GE.^{17,36-39} Moreover, when NES-1 was administered to HFD-fed rats at 10 to 20-times higher doses than our NES-1 dose, it was effective in inhibiting GE,⁴⁰ suggesting that the effect of NES-1 is dose-dependent and HFD could be elevating the threshold for its suppressive action on GE. Central administration of NES-1 was shown to activate efferent neurons in the dorsal motor nucleus of the vagus (DMNV), and directly stimulate cultured DMNV neurons,⁴¹ implicating the role of vagal efferents in the inhibitory effect of central NES-1 administration on gastric functions. In conscious dogs, using force transducers implanted onto the serosal surfaces throughout the GI tract, it was reported that intravenous administration of NES-1 reduced gastric contractions and inhibited cyclical interdigestive migrating contractions.⁴² In accordance with our results demonstrating that HFD eliminates the inhibitory role of NES-1 on GE, it was shown in an *in vitro* model of gastric vagal afferent preparation that the ability of NES-1 in potentiating the mechanosensitivity of gastric tension receptors and mucosal vagal afferents has disappeared when mice were fed with HFD.⁴³ There is convincing data showing that serum concentrations or tissue NUCB2 mRNA expressions were elevated in obese mice or patients,^{44,45} while expressions of NUCB2 mRNA and NES-1 in gastric and adipose tissue depots as well as circulating NES-1 levels were increased when animals were fed with HFD,⁴⁶ suggesting a compensatory upregulation of NES-1 synthesis. When taken together with the aforementioned studies, our findings implicate that HFD weakens the inhibitory effect of NES-1, and centrally released or administered NES-1, which appears to operate by the cross-talk of CCK and GLP-1 receptors, becomes incapable of controlling the gastric motility. It can be further suggested that the loss of this nesfatin-induced prolongation of food stay in the stomach and the accompanying reduction in satiety may further contribute to the progress of obesity.

Fat in the diet or its intraduodenal administration suppresses perceptions of appetite and stimulates the secretion of CCK and GLP-1,⁴⁷⁻⁵⁰ both of which delay GE, reduce gastric accommodation and food intake by inhibiting vagal-cholinergic function.⁵¹⁻⁵⁴ CCK and GLP-1 were shown to be co-localized with NUCB2/NES-1 in the intestinal mucosa⁵⁵⁻⁵⁷ and intestinal CCK mRNA expression in mice was upregulated by the infusion of NES-1,⁵⁶ implicating the co-function of NES-1 with both CCK and GLP-1. On the other hand, HFD was shown to diminish the inhibitory effect of fat and CCK in delaying GE⁵⁸ and postprandial secretion of GLP-1 was decreased with the development of obesity.⁵⁹ In support of these reports, our data demonstrated that the immediate inhibitory effect of centrally applied NES-1 on non-nutrient emptying was reversed by CCK-1, CCK-2, and GLP-1 receptor antagonists, but this interrelated inhibition was abolished in HFD-fed rats. Since the inhibitory effect of NES-1 was not observed in either the gastric or ileal smooth muscles, it could be postulated that the inhibition is regulated by the neuronal (ie, vagal) control mechanisms via the activity of CCK and GLP-1 receptors. Moreover, the stimulatory effect of HFD on gastric contractility appears to be overridden by a possible inhibitory enterogastric reflex mediated by an interaction between NES-1, CCK, and GLP-1 receptors.

Researchers have identified multiple intersections between the controlling mechanisms of nutrient metabolism, obesity and inflammation, and the term “meta-inflammation” was coined to illustrate the occurrence of a low-grade inflammation in response to obesity.⁶⁰⁻⁶² As a consequence of meta-inflammation, consumption of the pro-inflammatory HFD was shown to initiate apoptotic damage and the loss of hypothalamic, enteric, and extrinsic (mainly vagal) neurons,^{63,64} resulting in obesity-related GI dysfunction,^{65,66} which further alters food intake, energy balance, and exacerbates the severity of obesity.^{67,68} In addition to our previous study showing that a low-level of hepatointestinal inflammation was accompanied by delayed intestinal transit,⁶⁹ our current results also confirmed that HFD feeding has resulted in increased reactive oxygen metabolite generation and histologically proven mild inflammation in the liver and intestines, while increased gastric contractility, loss of NES-1-induced hypomotility, and depressed intestinal contractility were accompanied by HFD-induced alterations in the immunoreactivity of enteric neurotransmitters. In parallel to those shown in the intestines of mice,⁷⁰ we also observed that feeding with HFD increased gastric nNOS immunoreactive neurons, which are mostly inhibitory motor neurons; while nNOS immunoreactivity was reduced in the intestinal nerve plexuses of HFD-fed rats. Our findings also revealed that VIP immunoreactivity and TH immunoreactivity were

reduced in the gastric myenteric plexus, but both immunoreactivities were enhanced in the intestinal layers. Similarly, it was demonstrated that VIP varicosities were decreased in the duodenum and ileum of HFD-fed mice.⁷¹ In contrary, a reduction was observed in the antral and duodenal VIPergic neurons of obese diabetic mice.⁷² Although it cannot be explained yet how HFD affects the intertwined signaling pathways of VIP, dopamine, norepinephrine, and nNOS, it can be suggested that the differences in species, duration of exposure to HFD, and different segments of the GI tract could be responsible of HFD-associated conflicting changes in gut neuronal network and the resultant alterations in motility.

In the present study, we investigated the involvement of GLP-1 and CCK receptors in the gastromodulatory role of central NES-1. One of the limitations of our study was that the actions of NES-1 were not tested by the use of a specific NES-1 receptor antagonist. However, despite that autoradiographic studies showing that NES-1 binds to a variety of brain areas including DMNV nerve as well as the stomach and small intestines,⁷³ the NUCB2/NES-1 receptor is not yet identified. Thus, further studies with its specific antagonists are warranted upon the isolation of the NUCB2/NES-1 receptor. Due to the design of the experiments, we implemented the metabolic/biochemical measurements and the motility experiments in separate animal groups, therefore we could not directly perform any correlation analysis among the motility changes and the degree of HFD-induced inflammation.

In conclusion, the findings of the current study demonstrate for the first time that NES-1-induced delay in GE was mediated via the involvement of GLP-1, CCK-1, and CCK-2 receptors, and this inhibitory effect of NES-1 on GE rate was not evident upon prolonged consumption of HFD, which has disrupted the interbalance of enteric neurotransmitters. Based on the current results, one of the future challenges in targeting the treatment of obesity would be to unravel whether the central expressions of NUCB2/NES-1 receptor change in response to HFD feeding and obesity.

Acknowledgements: Authors are grateful to Nişva Hilal Sağlam for her support in the preparation of the histological samples. The results were partially presented at Europhysiology 2018 in London, UK.

Financial support: None.

Conflicts of interest: None.

Author contributions: The experiments were performed at the Marmara University School of Medicine, Departments of Physiology and Histology, and Marmara University Vocational School of

Health Sciences. All persons who qualify for authorship are listed. All authors agree to be accountable for all aspects of the work in ensuring that questions related to the accuracy or integrity of any part of the work are appropriately investigated and resolved. Study conception and design of the work: Berrak Ç Yeğen; data acquisition: Zarife N Özdemir-Kumral, Türkan Koyuncuoğlu, and Sevil Arabacı-Tamer; analysis and data interpretation, drafting of the manuscript, and approval of the final version of the manuscript: Zarife N Özdemir-Kumral, Türkan Koyuncuoğlu, Sevil Arabacı-Tamer, Özlem T Çilingir-Kaya, Ayça K Köroğlu, Meral Yüksel, and Berrak Ç Yeğen; and critical revision: Berrak Ç Yeğen.

References

1. Keller J, Bassotti G, Clarke J, et al. Expert consensus document: advances in the diagnosis and classification of gastric and intestinal motility disorders. *Nat Rev Gastroenterol Hepatol* 2018;15:291-308.
2. Mushref MA, Srinivasan S. Effect of high fat-diet and obesity on gastrointestinal motility. *Ann Transl Med* 2013;1:14.
3. Castiglione KE, Read NW, French SJ. Adaptation to high-fat diet accelerates emptying of fat but not carbohydrate test meals in humans. *Am J Physiol Integr Comp Physiol* 2002;282:R366-R371.
4. Martinez-Guryn K, Hubert N, Frazier K, et al. Small intestine microbiota regulate host digestive and absorptive adaptive responses to dietary lipids. *Cell Host Microbe* 2018;23:458-469, e5.
5. Delgado-Aros S, Cremonini F, Castillo JE, et al. Independent influences of body mass and gastric volumes on satiation in humans. *Gastroenterology* 2004;126:432-440.
6. Park JH, Kwon OD, Ahn SH, Lee S, Choi BK, Jung KY. Fatty diets retarded the propulsive function of and attenuated motility in the gastrointestinal tract of rats. *Nutr Res* 2013;33:228-234.
7. Li J, Ma W, Wang S. Slower gastric emptying in high-fat diet induced obese rats is associated with attenuated plasma ghrelin and elevated plasma leptin and cholecystokinin concentrations. *Regul Pept* 2011;171:53-57.
8. Rivera LR, Leung C, Pustovit RV, et al. Damage to enteric neurons occurs in mice that develop fatty liver disease but not diabetes in response to a high-fat diet. *Neurogastroenterol Motil* 2014;26:1188-1199.
9. Voss U, Sand E, Olde B, Ekblad E. Enteric neuropathy can be induced by high fat diet *in vivo* and palmitic acid exposure *in vitro*. *PLoS One* 2013;8:e81413.
10. Wood JD, Kirchgessner A. Slow excitatory metabotropic signal transmission in the enteric nervous system. *Neurogastroenterol Motil* 2004;16(suppl 1):71-80.
11. Stenkamp-Strahm CM, Nyavor YE, Kappmeyer AJ, Horton S, Gericke M, Balemba OB. Prolonged high fat diet ingestion, obesity, and type 2 diabetes symptoms correlate with phenotypic plasticity in myenteric neurons and nerve damage in the mouse duodenum. *Cell Tissue Res* 2015;361:411-426.
12. Oh I, Shimizu H, Satoh T, et al. Identification of nesfatin-1 as a satiety

- molecule in the hypothalamus. *Nature* 2006;443:709-712.
13. Brailoiu GC, Dun SL, Brailoiu E, et al. Nesfatin-1: distribution and interaction with a G protein-coupled receptor in the rat brain. *Endocrinology* 2007;148:5088-5094.
 14. Foo KS, Brismar H, Broberger C. Distribution and neuropeptide coexistence of nucleobindin-2 mRNA/nesfatin-like immunoreactivity in the rat CNS. *Neuroscience* 2008;156:563-579.
 15. Zhang AQ, Li XL, Jiang CY, et al. Expression of nesfatin-1/NUCB2 in rodent digestive system. *World J Gastroenterol* 2010;16:1735-1741.
 16. Kohno D, Nakata M, Maejima Y, et al. Nesfatin-1 neurons in paraventricular and supraoptic nuclei of the rat hypothalamus coexpress oxytocin and vasopressin and are activated by refeeding. *Endocrinology* 2008;149:1295-1301.
 17. Stengel A, Goebel M, Yakubov I, et al. Identification and characterization of nesfatin-1 immunoreactivity in endocrine cell types of the rat gastric oxyntic mucosa. *Endocrinology* 2009;150:232-238.
 18. Li Z, Xu G, Li Y, Zhao J, Mulholland MW, Zhang W. mTOR-dependent modulation of gastric nesfatin-1/NUCB2. *Cell Physiol Biochem* 2012;29:493-500.
 19. Finelli C, Martelli G, Rossano R, et al. Nesfatin-1: role as possible new anti-obesity treatment. *EXCLI J* 2014;13:586-591.
 20. Stengel A, Goebel M, Wang L, et al. Central nesfatin-1 reduces dark-phase food intake and gastric emptying in rats: differential role of corticotropin-releasing factor2 receptor. *Endocrinology* 2009;150:4911-4919.
 21. Paxinos, George, Charles Watson. *The Rat Brain, in Stereotaxic Coordinates*. San Diego: Academic Press 1997.
 22. Scarpignato C, Tangwa M, Tramacere R, Del Soldato P. The effect of the new H2-receptor antagonist mifentidine on gastric secretion, gastric emptying and experimental gastric and duodenal ulcers in the rat: comparison with cimetidine and ranitidine. *Digestion* 1986;33:7-16.
 23. Debas HT, Farooq O, Grossman MI. Inhibition of gastric emptying is a physiological action of cholecystokinin. *Gastroenterology* 1975;68(5 Pt 1):1211-1217.
 24. Green T, Dimaline R, Peikin S, Dockray GJ. Action of the cholecystokinin antagonist L364, 718 on gastric emptying in the rat. *Am J Physiol* 1988;255(5 Pt 1):G685-G689.
 25. Gürler EB, Özbeyli D, Buzcu H, et al. Natural sweetener agave inhibits gastric emptying in rats by a cholecystokinin-2-and glucagon like peptide-1 receptor-dependent mechanism. *Food Funct* 2017;8:741-745.
 26. Bradley P, Priebe DA, Christensen RD, Rothstein G. Measurement of cutaneous inflammation: estimation of neutrophil content with an enzyme marker. *J Invest Dermatol* 1982;78:206-209.
 27. Ohkawa H, Ohishi N, Yagi K. Assay for lipid peroxides in animal tissues by thiobarbituric acid reaction. *Anal Biochem* 1979;95:351-358.
 28. Ellman GL. Tissue sulphhydryl groups. *Arch Biochem Biophys* 1959;82:70-77.
 29. Krol W, Czuba Z, Scheller S, Gabrys J, Grabiec S, Shani J. Anti-oxidant property of ethanolic extract of propolis (EEP) as evaluated by inhibiting the chemiluminescence oxidation of luminol. *Biochem Int* 1990;21:593-597.
 30. Deshpande SS. Principles and applications of luminescence spectroscopy. *Crit Rev Food Sci Nutr* 2001;41:155-224.
 31. Gibson-Corley KN, Olivier AK, Meyerholz DK. Principles for valid histopathologic scoring in research. *Vet Pathol* 2013;50:1007-1015.
 32. Kim DY, Camilleri M, Murray JA, Stephens DA, Levine JA, Burton DD. Is there a role for gastric accommodation and satiety in asymptomatic obese people? *Obes Res* 2001;9:655-661.
 33. Hayashi Y, Toyomasu Y, Saravanaperumal SA, et al. Hyperglycemia increases interstitial cells of cajal via MAPK1 and MAPK3 signaling to ETV1 and KIT, leading to rapid gastric emptying. *Gastroenterology* 2017;153:521-535, e20.
 34. Mathus-Vliegen EM, Van Ierland-Van Leeuwen ML, Roolker W. Gastric emptying, CCK release, and satiety in weight-stable obese subjects. *Dig Dis Sci* 2005;50:7-14.
 35. Di Ciaula A, Wang DQ, Portincasa P. Gallbladder and gastric motility in obese newborns, pre-adolescents and adults. *J Gastroenterol Hepatol* 2012;27:1298-1305.
 36. Atsuchi K, Asakawa A, Ushikai M, et al. Centrally administered nesfatin-1 inhibits feeding behaviour and gastroduodenal motility in mice. *Neuroreport* 2010;21:1008-1011.
 37. Gao S, Guo F, Sun X, Zhang N, Gong Y, Xu L. The inhibitory effects of nesfatin-1 in ventromedial hypothalamus on gastric function and its regulation by nucleus accumbens. *Front Physiol* 2017;7:634.
 38. Xu L, Wang H, Gong Y, et al. Nesfatin-1 regulates the lateral hypothalamic area melanin-concentrating hormone-responsive gastric distension-sensitive neurons and gastric function via arcuate nucleus innervation. *Metabolism* 2017;67:14-25.
 39. Xu L, Wang Q, Guo F, et al. Nesfatin-1 signaling in the basomedial amygdala modulates the gastric distension-sensitive neurons discharge and decreases gastric motility via melanocortin 3/4 receptors and modified by the arcuate nucleus. *Eur J Pharmacol* 2015;764:164-172.
 40. Yang GT, Zhao HY, Kong Y, Sun NN, Dong AQ. Study of the effects of nesfatin-1 on gastric function in obese rats. *World J Gastroenterol* 2017;23:2940-2947.
 41. Xia ZF, Fritze DM, Li JY, et al. Nesfatin-1 inhibits gastric acid secretion via a central vagal mechanism in rats. *Am J Physiol Gastrointest Liver Physiol* 2012;303:G570-G577.
 42. Watanabe A, Mochiki E, Kimura A, et al. Nesfatin-1 suppresses gastric contractions and inhibits interdigestive migrating contractions in conscious dogs. *Dig Dis Sci* 2015;60:1595-1602.
 43. Kentish SJ, Li H, Frisby CL, Page AJ. Nesfatin-1 modulates murine gastric vagal afferent mechanosensitivity in a nutritional state dependent manner. *Peptides* 2017;89:35-41.
 44. Mohan H, Ramesh N, Mortazavi S, Le A, Iwakura H, Unniappan S. Nutrients differentially regulate nucleobindin-2/nesfatin-1 *in vitro* in cultured stomach ghrelinoma (MGN3-1) cells and *in vivo* in male mice. *PLoS One* 2014;9:e115102.
 45. Samani SM, Ghasemi H, Bookani KR, Shokouhi B. Serum nesfatin-1 level in healthy subjects with weight-related abnormalities and newly diagnosed patients with type 2 diabetes mellitus; a case-control study. *Acta Endocrinol(Buchar)* 2019;15:69-73.
 46. Ramanjaneya M, Chen J, Brown JE, et al. Identification of nesfatin-1 in human and murine adipose tissue: a novel depot-specific adipokine with increased levels in obesity. *Endocrinology* 2010;151:3169-3180.

47. Arora S, Anubhuti. Role of neuropeptides in appetite regulation and obesity—a review. *Neuropeptides* 2006;40:375–401.
48. Bagger JI. Physiological and pathophysiological aspects of incretin hormones and glucagon. *Dan Med J* 2017;64:B5331.
49. Little TJ, Russo A, Meyer JH, et al. Free fatty acids have more potent effects on gastric emptying, gut hormones, and appetite than triacylglycerides. *Gastroenterology* 2007;133:1124–1131.
50. Stewart JE, Feinle-Bisset C, Keast RS. Fatty acid detection during food consumption and digestion: associations with ingestive behavior and obesity. *Prog Lipid Res* 2011;50:225–233.
51. Chaudhri O, Small C, Bloom S. Gastrointestinal hormones regulating appetite. *Philos Trans R Soc Lond B Biol Sci* 2006;361:1187–1209.
52. Delgado-Aros S, Kim DY, Burton DD, et al. Effect of GLP-1 on gastric volume, emptying, maximum volume ingested, and postprandial symptoms in humans. *Am J Physiol Gastrointest Liver Physiol* 2002;282:G424–G431.
53. McMenamin CA, Travagli RA, Browning KN. Inhibitory neurotransmission regulates vagal efferent activity and gastric motility. *Exp Biol Med*(Maywood) 2016;241:1343–1350.
54. Miyasaka K, Ohta M, Kanai S, et al. Enhanced gastric emptying of a liquid gastric load in mice lacking cholecystokinin-B receptor: a study of CCK-A, B, and AB receptor gene knockout mice. *J Gastroenterol* 2004;39:319–323.
55. Ramesh N, Mortazavi S, Unniappan S. Nesfatin-1 stimulates glucagon-like peptide-1 and glucose-dependent insulinotropic polypeptide secretion from STC-1 cells *in vitro*. *Biochem Biophys Res Commun* 2015;462:124–130.
56. Ramesh N, Mortazavi S, Unniappan S. Nesfatin-1 stimulates cholecystokinin and suppresses peptide YY expression and secretion in mice. *Biochem Biophys Res Commun* 2016;472:201–208.
57. Schalla MA, Unniappan S, Lambrecht NWG, Mori M, Taché Y, Stengel A. NUCB2/nesfatin-1-Inhibitory effects on food intake, body weight and metabolism. *Peptides* 2020:170308.
58. Covasa M, Ritter RC. Adaptation to high-fat diet reduces inhibition of gastric emptying by CCK and intestinal oleate. *Am J Physiol Regul Integr Comp Physiol* 2000;278:R166–R170.
59. Verdich C, Toubro S, Buemann B, Madsen JL, Holst JJ, Astrup A. The role of postprandial releases of insulin and incretin hormones in meal-induced satiety-effect of obesity and weight reduction. *Int J obes Relat Metab Disord* 2001;25:1206–1214.
60. Hotamisligil GS. Inflammation and metabolic disorders. *Nature* 2006;444:860–867.
61. Li H, Lelliott C, Håkansson P, et al. Intestinal, adipose, and liver inflammation in diet-induced obese mice. *Metabolism* 2008;57:1704–1710.
62. Lumeng CN, Saltiel AR. Inflammatory links between obesity and metabolic disease. *J clin Invest* 2011;121:2111–2117.
63. Khiaosa-Ard R, Zebeli Q. Diet-induced inflammation: from gut to metabolic organs and the consequences for the health and longevity of ruminants. *Res Vet Sci* 2018;120:17–27.
64. Moraes JC, Coope A, Morari J, et al. High-fat diet induces apoptosis of hypothalamic neurons. *PLoS One* 2009;4:e5045.
65. McMenamin CA, Clyburn C, Browning KN. High-fat diet during the perinatal period induces loss of myenteric nitrergic neurons and increases enteric glial density, prior to the development of obesity. *Neuroscience* 2018;393:369–380.
66. Nezami BG, Mwangi SM, Lee JE, et al. MicroRNA 375 mediates palmitate-induced enteric neuronal damage and high-fat diet-induced delayed intestinal transit in mice. *Gastroenterology* 2014;146:473–483.e3.
67. Berthoud HR. The vagus nerve, food intake and obesity. *Regul Pept* 2008;149:15–25.
68. Yavuz Y, Kumral ZN, Memi G, Çevik ÖD, Yeğen C, Yeğen BÇ. Serum leptin, obestatin, and ghrelin levels and gastric emptying rates of liquid and solid meals in non-obese rats with roux-en-Y bypass surgery or prosthesis placement: implications for the role of vagal afferents. *Obes Surg* 2017;27:1037–1046.
69. Yıldırım A, Tamer SA, Sahin D, et al. The effects of antibiotics and melatonin on hepato-intestinal inflammation and gut microbial dysbiosis induced by a short-term high-fat diet consumption in rats. *Br J Nutr* 2019;122:841–855.
70. Qu ZD, Thacker M, Castelucci P, Bagyánszki M, Epstein ML, Furness JB. Immunohistochemical analysis of neuron types in the mouse small intestine. *Cell Tissue Res* 2008;334:147–161.
71. Soares A, Beraldi EJ, Ferreira PE, Bazotte RB, Buttow NC. Intestinal and neuronal myenteric adaptations in the small intestine induced by a high-fat diet in mice. *BMC Gastroenterol* 2015;15:3.
72. Spångéus A, El-Salhy M. Myenteric plexus of obese diabetic mice (an animal model of human type 2 diabetes). *Histol Histopathol* 2001;16:159–165.
73. Prinz P, Goebel-Stengel M, Teuffel P, Rose M, Klapp BF, Stengel A. Peripheral and central localization of the nesfatin-1 receptor using autoradiography in rats. *Biochem Biophys Res Commun* 2016;470:521–527.